

II. MEASUREMENT TECHNIQUES

- A. Gas Counting**
- B. Liquid Scintillation Counting**
- C. Accelerator Mass Spectrometry**
- D. Standardization, Intercomparison, Data management**

ON THE VALIDITY OF THE POISSON HYPOTHESIS FOR LOW-LEVEL COUNTING: INVESTIGATION OF THE DISTRIBUTIONAL CHARACTERISTICS OF BACKGROUND RADIATION WITH THE NIST INDIVIDUAL PULSE COUNTING SYSTEM¹

L. A. CURRIE,² E. M. EIJGENHUIJSEN³ and G. A. KLOUDA²

ABSTRACT. Does radioactive decay follow the Poisson distribution?—a fundamental question, to which the theoretical answer seems to be, Yes. On the practical side, the answer to this question impacts the best achievable precision in well-controlled counting experiments. There have been some noteworthy experimental tests of the Poisson assumption, using systems carefully designed for the analysis of individual pulses from stable radioactive sources; thus far, experiment supports theory. For low-level counting, the nature of the background distribution can be of profound practical importance, especially for very long counting experiments where validation by an adequate number of full replicates may be impracticable. One is tempted in such cases to assume that the variance is equal to the mean, in order to estimate the measurement uncertainty. Background radiation, however, has multiple components, only some of which are governed by the laws of radioactive decay.

A specially designed low-level gas counting system at NIST for interactive, retrospective individual pulse shape and time series analysis makes possible the investigation of the empirical distribution function of the background radiation, in a manner similar to the previous empirical distribution studies of radioactive decay. Benefits of individual pulse analysis are that there is no information loss due to averaging and that two independent tests of the Poisson hypothesis can be performed using data from a single, extended measurement period without the need for replication; namely, tests of the distribution of arrival times, expected to be uniform, and the distribution of inter-arrival times, expected to be exponential. For low-level counting the second test has a very interesting and very informative complement: the distribution of coincidence-anticoincidence inter-arrival times.

Key outcomes from the study were that: 1) nonstationarity in the mean background rate over extended periods of time could be compensated by an on-line paired counter technique, which is far preferable to the questionable practice of using an “error-multiplier” that presumes the wandering (nonstationary) background to be random; and 2) individual empirical pulse distributions differed from the ideal GM and Poisson processes by exhibiting giant pulses, a continuum of small pulses, afterpulses, and in certain circumstances bursts of pulses and transient relaxation processes. The afterpulses constituted ca. 8% of the anti-coincidence background events, yet they *escaped detection* by the conventional distributional tests.

INTRODUCTION

Motivation

For theoretical reasons, as well as for practical ones related to the treatment of counting “error” (uncertainty), there has long been an interest in the experimental verification of the Binomial-Poisson hypothesis for radioactive decay (Berkson 1975; Cannizzaro *et al.* 1978; Curtiss 1930; Garfinkel and Mann 1968). For measurements in which background is dominant, or at least non-negligible, it is equally important to investigate the distribution of the background radiation. Such knowledge is mandatory for the estimation of detection and quantification limits, as well as for setting meaningful uncertainty intervals for estimated net signals. Previous distributional studies of radioactive decay lend support to the assumption that that portion of the background due to long-lived radionuclide contaminants would follow the Poisson distribution; this does not automatically follow, however, for all other background components. That leads to the objective of the work reported here: to perform an evaluation of the distribution of the background radiation, specifically for the case of low-level gas counting (Cook *et al.* 1992; Kaihola, Polach and Kojola 1984; Mook 1982; Theodórsson 1992). This endeavor is interesting for several reasons. First, the background is rarely negligible in such

¹Contribution of the National Institute of Standards and Technology; not subject to copyright.

²Chemical Science and Technology Laboratory, National Institute of Standards and Technology (NIST), Gaithersburg, Maryland 20899 USA

³Sandoz Pharma AG, Bau 360/816, CH-4000 Basel, Switzerland

systems, and frequently uncertainty and/or variability associated with the background radiation is limiting, overshadowing that arising from procedural blanks. Second, for extended measurement times, it may be difficult or impracticable to collect the large number of background replicates needed to develop a precise estimate of its variability, much less assess the nature of its distribution. Background stability over long periods of time required for such a test compounds the problem. Third, the anticoincidence technique for background suppression makes low-level counting especially susceptible to certain types of deviations from the Poisson hypothesis (Currie *et al.* 1997). Background instability—*i.e.*, changes in the mean level of the background radiation over time (non-stationarity), will be considered briefly, but that is not the prime focus of this investigation.

The Case for the Poisson Distribution

The Poisson distribution is perhaps the single, most important distribution describing the occurrence of random events. It is by no means restricted to long-lived radioactive decay, but may apply to numerous other random phenomena in the physical, biological and social sciences, ranging from the occurrence of natural disasters, to the appearance of pulses along a nerve fiber, to “white noise” in chemical sensors, to reactions in molecular and nuclear beams. The underlying requirement is that individual events in a series occur at random with a fixed probability (rate) of occurrence (Cox and Lewis 1968).⁴ This discrete distribution has but one parameter, such that the variance is equal to the mean; hence, an estimate for the standard deviation, and of confidence intervals follow automatically from an estimate of the mean. In fact, the ratio of the variance of counting data to the mean, known as the “index of dispersion,” serves as one of the tests for the Poisson distribution. Another fundamental property is the existence of the three manifestations or equivalent distributions when the Poisson hypothesis is satisfied: 1) the Poisson distribution of counts, 2) the Uniform distribution of arrival (occurrence) times, and 3) the Exponential distribution of inter-arrival times. The ability to test an experimental series of events against all three manifestations permits us to investigate deviations, having different physicochemical causes, from the null (Poisson) hypothesis. To achieve that, one must have the capability of identifying individually each event in the series being tested. The unique NIST low-level counting system makes that possible by labeling each count with its time of arrival (Currie *et al.* 1983; Eijgenhuijsen *et al.* 1996).

Observables and Net Signals

Investigation of the background radiation necessarily requires an observing device—in this study, a low-level gas counting system. What we observe, therefore, is the convolution of the “true” background distribution and artifacts introduced by the observing system.⁵ As we shall see later, low-level (anticoincidence) counting is especially vulnerable to certain types of artifacts. To proceed, we are forced to specify the counting system and its parameters. Since GM counting was specified for this particular study, the null hypothesis is extended to include constant amplitude (“energy”) for all counting pulses; and the “deadtime” artifact immediately introduces a deviation from the ideal Poisson distribution (Jordan and McBeth 1978).

A second consideration is the fact that the results of counting experiments must always be expressed in terms of *differences* or net signals; the probability distribution of the differences is therefore of

⁴Cox and Lewis (p.18.6): “The Poisson process is a mathematical concept and no real phenomenon can be expected to be exactly in accord with it.”

⁵The observing (measurement) system can have a profound impact: one of the more extensive tests of the Poisson distribution for radioactive decay showed significant deviations from the Poisson hypothesis—later found to be the result of instrumental artifacts (Berkson 1975; Cannizzaro *et al.* 1978).

central importance. This issue is infamous in the case of very few counts, as the distribution of the difference between two Poisson distributed variables is no longer Poisson (Nicholson 1966). Attention to this matter is quite important also in the many count situation, where the Normal approximation to the Poisson distribution applies, as will be shown later in the treatment of serial vs. parallel (“on-line”) sample and background measurements.

COUNTING SYSTEM AND EXPERIMENTAL STRATEGY

The NIST low-level gas counting system, which permits recording and archiving of arrival times and complete waveforms of individual coincidence and anticoincidence pulses occurring in multiple Geiger-Müller (GM) or proportional counting tubes, is described elsewhere (Eijgenhuijsen *et al.* 1996).⁶ The system provides 1 μ s pulse pair time resolution, which is <1% of the inherent time resolution (deadtime) of the GM counters, and negligible compared to the mean interval (*ca.* 3 s) between coincidence events. The time devoted to the entire study amounted to *ca.* six weeks, with *ca.* twenty 0.7- to 3-day individual counting periods for each of two, 45 mL GM counters operating in parallel. The total number of background events (coincidence + anticoincidence) collected was in excess of 1.4 million. Figure 1 shows, for our pair of Cu-cathode, Ar-(C₂H₅)₂O filled counters, the superposition of the actual GM coincidence waveforms collected during one of the measurement periods (top), and a 150 s individual pulse data stream from the same experiment (bottom). (The single, “giant” pulse that occurred during this experiment appears in both records.)

Hypotheses concerning the background distribution and GM pulse amplitudes were evaluated with a series of “external” and “internal” tests. *External tests* used coincidence and anticoincidence background counting rate data from 21 independent (“serial”) counting periods and 18 dual counter (“parallel”) counting periods using Poisson weighted residuals to evaluate the index of dispersion and $p(\chi^2)$. *Internal tests* used the full set of individual pulse data from single counting periods to compare the empirical distributions of pulse amplitudes, counts, arrival times, and inter-arrival times with the predictions of the Poisson and GM counting processes. Internal tests were extended also to two special cases involving “stressed” and “shocked” GM counting tubes.

EXPERIMENTAL DATA; RESULTS OF DISTRIBUTIONAL TESTS

To set the stage for the discussion of test results, and to introduce some notation, we refer to the pulse data stream shown in Figure 1b. Two dimensions are shown: the x-axis, spanning a period of 150 s in the figure, indicates the time of arrival of the individual pulses; the z-axis shows the pulse amplitude ($E = \text{“energy”}$), covering a range 0 to 10 volts (amplifier saturation). One of the pulses is labeled “G” for giant; two are labeled “A” for anticoincidence; the remainder are of type “C” (coincidence). Inter-arrival times are of two types: “dt,” the interval between an “A” and the preceding “C” pulse; “DT,” the interval between two sequential “A” pulses. The figure highlights several possible distributional tests: 1) GM pulse amplitude (“E”) distribution; 2) arrival time distribution (position on the x-axis); 3) “A-A,” anticoincidence interval distribution; and 4) “A-C,” anticoincidence-coincidence interval distribution, of peculiar importance to low-level counting (Currie *et al.* 1997). Other tests addressed: 5) the Poisson distribution of counts obtained by integrating over equal, very short periods of time; and 6) the independence of successive inter-arrival times, or more generally the noise power spectrum, which is expected to be “white” for a Poisson process.

⁶See the Postscript to this paper for a brief description of coincidence-anticoincidence counting.

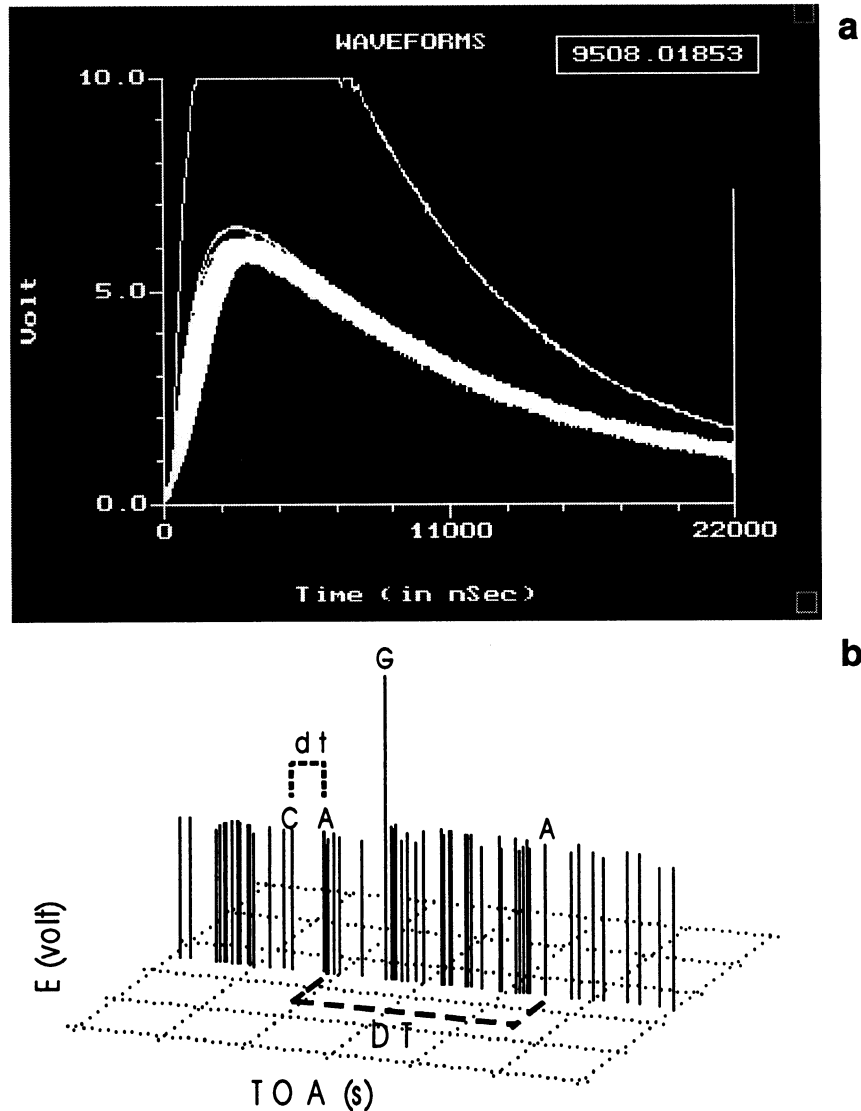


Fig. 1. Low-level GM individual pulse shape (waveform) and time series characteristics. **1a** (top): Superposition of coincidence pulse waveforms collected during one of the extended counting periods, showing the approximately constant pulse amplitude (expected) for GM pulses, with one notable exception. (The number at the top of the waveform display (Fig. 1a) represents the time of arrival of the final event, 9508.01853 s). **1b** (bottom): A 150-s snapshot of the individual pulse data stream from the same counting period, showing in the x-z plane, the actual distribution of pulse times of arrival (TOA) and pulse amplitudes (E). (The y-axis has been reserved for pulse shape data.) This figure gives the notation used in this study, with the indication of three types of events: a (rare) giant pulse (G); two anticoincidence pulses (A); and the remainder being coincidence pulses (C). DT represents the interval between successive anticoincidence background events, while dt represents the interval between anticoincidence events and preceding (coincidence) events.

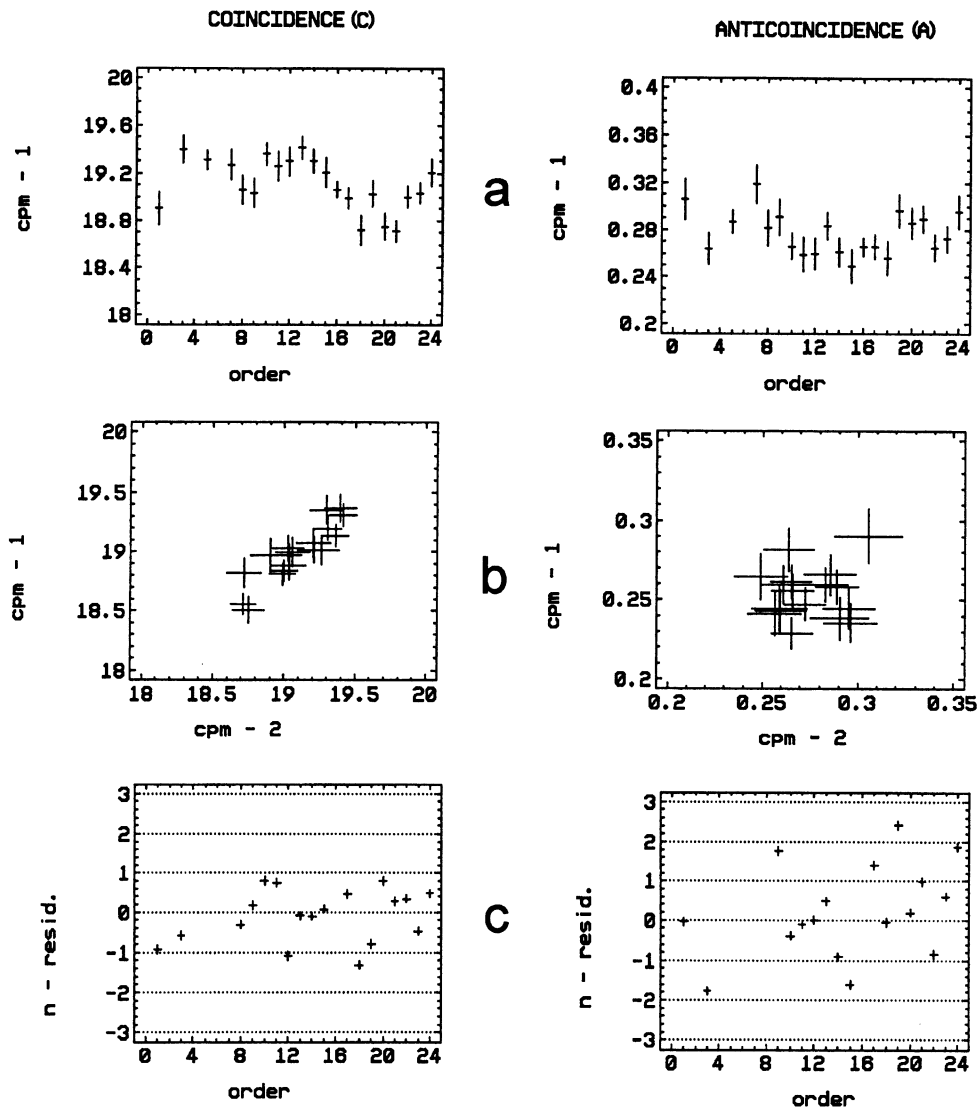


Fig. 2. *External tests* of the distribution of background events, over a time of *ca.* 6 weeks, divided into 24 more-or-less equal counting periods, some with missing data. **2a** (top): Extended measurements of coincidence (C) and anti-coincidence (A) background rates for counter-1 (cpm-1), showing variations about the weighted means and weighted Poisson- σ 's. Nonstationarity (changing mean rate) for the C-data was indicated both visually, and by the large value for index of dispersion (I) and the poor fit ($p < 0.000001$) to the simple Poisson model. Also, the A-data were barely consistent with the model ($p = 0.019$). **2b** (center): Covariation of the extended counting data for the paired counters 1 and 2 (cpm-1 vs. cpm-2). The correlation coefficient for the C-results was 0.90 ($p < 0.0001$); for the A-results it was non-significant at 0.13 ($p = 0.62$). **2c** (bottom): Poisson-weighted normalized residual plots for the differences between paired counter background measurements, as a test for long-term background nonstationarity compensation with an on-line background counter. Residuals are shown about the weighted mean differences of 0.11 cpm (C-events) and 0.021 cpm (A-events). For the C-events, the fit was a little "too good," with index of dispersion less than one ($I = 0.44$, $p = 0.975$), suggesting lack of independence between the C-events in the dual counters. For the A-events the fit was acceptable ($I = 1.46$, $p = 0.10$).

GM Pulse Amplitude Distribution

GM pulses are reputed to be all of approximately equal amplitude and shape (waveform), with a fixed mean amplitude which itself increases with voltage or position on the plateau. With the interesting exception of the rare, giant pulse, Figure 1 supports that assumption for the experimental data displayed there. Figure 1a shows the similarity in amplitude and shape for the full series of 2940 pulses; the similarity and scatter of the pulse energy can be seen also in the 150 s fragment shown in Figure 1b. More extensive tests were performed on the energy distributions of coincidence pulses and anticoincidence pulses collected during a 982-min background measurement on 29 April 1997. The estimated relative standard deviations were *ca.* 3.4% and 13% for the coincidence and anticoincidence pulse amplitude distributions, respectively. The latter showed more asymmetry, and skew toward lower amplitude pulses. In other work we have identified the smaller pulses, with the help of their pulse arrival time signatures, as spurious “afterpulses,” which occur rarely but regularly in GM counting tubes (Currie *et al.* 1997). (The relative immunity of coincidence counts to afterpulses is a result of their rare and random occurrence in individual counters [Narita *et al.* 1979].) Thus, at least two classes of pulses, afterpulses and the giant pulses of Figure 1 (Kern 1963) depart from the traditional expectation of constant pulse amplitude for GM counting. Neither giant pulses nor afterpulses are new discoveries in GM counting, but this *may be the first time that they have been documented in low-level counting background*. The afterpulsing phenomenon cannot be ignored in very high precision low-level (GM) counting, but the giant pulses, which are accompanied by interesting after effects, are quite rare. A summary of time constants for these and other artifacts observed in this study are given at the end of this paper.

External Distributional Tests

Two counters were employed for a series of *ca.* 20 long-term (0.7 to 3 day) counts in order to test the Poisson distribution of counts over an extended period of time (*ca.* 6 weeks). We show the results of these tests in a set of three pairs of plots. The first, Figure 2a, displays the observed rates and Poisson standard errors for 21 of these long-term background counts in counting channel 1. The obvious visual departures from stationarity (constant mean rate) is supported numerically by the values of χ^2 for the Poisson weighted residuals from the weighted means. For the coincidence counts, $p(\chi^2) < 0.000001$; for the anticoincidence counts, $p(\chi^2) = 0.019$. The equivalent values for the index of dispersion (I) are 4.9 and 1.8, respectively. This index, which is equivalent to the (variance/mean) ratio, should be unity for a Poisson process (Cox and Lewis 1968).

Figure 2b shows the relation between the extended counts for the dual counters in counting channels 1 and 2. The correlation is striking for the coincidence counts, but not statistically significant for the anticoincidence counts. The former is hardly surprising, for it has long been known that the muon (coincidence) intensity for low level counting varies inversely with barometric pressure because of muon interactions in the atmosphere; and the mean variation would necessarily be the same in each of the paired counters. (In fact, highly significant negative correlation of the coincidence rate with barometric pressure [$r = -.8$, $p < 0.0001$] was observed in this experiment.) Figure 2c addresses the issue of online background compensation, using the difference between paired sample-background counters for net signal estimation, as a means for *eliminating the effects of background nonstationarity*. Somewhat surprising results were obtained. For the anticoincidence counts the dispersion of the differences was reduced to a level consistent with Poisson “counting statistics” [$p(\chi^2) = 0.10$]—the intended outcome. For the coincidence counts, however, the dispersion of the differences was “too good”—*i.e.*, smaller than that predicted by Poisson counting statistics, with an index of dispersion less than unity (I = .44) and $p(\chi^2) = 0.975$. The implication is that the Poisson requirement of

independence was not satisfied for the paired counters for meson (coincidence) counting, perhaps as a result of meson showers, or secondary events in the shielding. By extension, if the anticoincidence background contains a residual cosmic ray component, the paired counter technique might lead to an overall variance somewhat smaller than that expected for the Poisson distribution.⁷

Internal Distributional Tests

More powerful tests of the background pulse distribution are possible by the “internal” route, in which the entire time series of individual pulses from a single counting period may be evaluated in terms of all three manifestations of the Poisson process—namely, the Poisson distribution of counts, the Uniform distribution of arrival times, and the Exponential distribution of inter-arrival times. Also, inter-arrival times are valuable for testing the assumption of independence using autocorrelation and noise spectral analysis. Assessment of the individual pulse data stream from these different perspectives is vital because of their complementary abilities to detect deviations from the Poisson process *arising from different physical causes*. To illustrate the methodology and develop initial information on deviations from the Poisson process, we shall use the 982-min time series of individual coincidence and anticoincidence background pulses derived from the dual counters on 29 April 1997. This series contained a total of 37,755 events, 98.4% of which were coincidence events.

Tests Based Strictly on the Anticoincidence Background Events

To test the *Poisson distribution of counts*, it is necessary to first aggregate events from the time series into a series of equal time windows (“bins”). This is followed by construction of a frequency histogram of counts. Figure 3a shows the result of the first operation, applied to the 585 anticoincidence events from the 29 April time series, using 400 successive bins. The number of bins is selected to make the average number of counts per bin sufficiently small to display the asymmetric Poisson character. The resulting histogram is shown in Figure 3b, together with the best fit Poisson distribution. The fit, with a mean of 1.46 counts is adequate [$p(\chi^2) = 0.11$].

Tests of the *Uniform distribution of arrival times* (TOA), and the *Exponential distribution of inter-arrival times* (DT) also may be performed using histogram formulations, where the events are aggregated into consecutive equal width bins or classes, with χ^2 as the test statistic. The results, for the same (29 April) anticoincidence pulse data series, are shown in Figure 3c and 4a, respectively. In the first case, the 585 arrival times have been grouped into 20 successive classes; the resulting frequency histogram (mean: 29.2 counts) is then compared to that expected for a uniform distribution. The fit is adequate, with $p(\chi^2) = 0.75$. In the second case, 584 inter-arrival times have been sorted into 50 equal DT classes between 0 and 1000 s, and compared to what would be expected for an exponential distribution. Here, too, the frequency histogram (Fig. 4a) is consistent with the null hypothesis, with $p(\chi^2) = 0.40$.

Histogram displays and χ^2 tests of classified (aggregated) data suffer two small drawbacks in terms of resolution loss and dependence on the level of aggregation (class width). An attractive alternative, which preserves the full resolution of the individual pulse data, utilizes the empirical cumulative frequency distribution functions (cdf). Maximum deviations of the empirical from the theoretical cdf are then tested with the Kolmogorov-Smirnov statistic (significance level: $p(K-S)$). Figure 3d shows the empirical and theoretical (uniform) cdf for the arrival times; Figure 4b,c shows the same for the (exponential) inter-arrival times. The results in each case are consistent with the respective null hypothesis.

⁷Residual cosmic-ray background components that occur in low-level gas counting include secondary gamma rays from muon interactions in the shield, neutrons, and “muon leakage” (Theodórsson 1992).

Not shown are the results of *autocorrelation and noise spectral analysis*, using both dt and DT inter-arrival times. In each case, the results obtained were consistent with “white noise” ($p[\text{dt}] = 0.88$, $p[\text{DT}] = 0.58$), as they must be if the underlying process is Poisson.

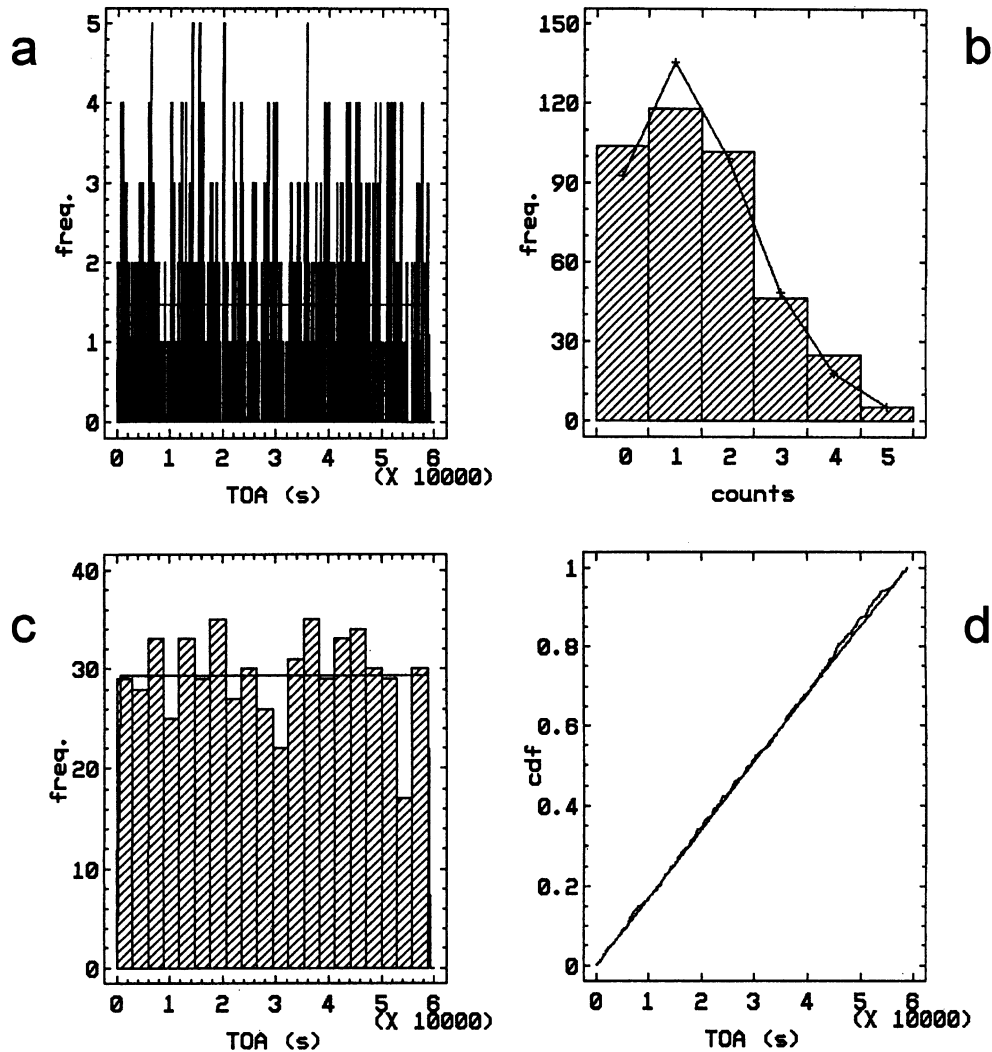


Fig. 3. *Internal tests of a single 982-min counting period (29 April 1997). Top: Test of the Poisson distribution of counts. 3a:* Partition of 585 anticoincidence events into 400 successive arrival time bins, used for the generation of the background count frequencies. *3b:* Resulting histogram showing the empirical and fitted Poisson distribution of counts ($I = 1.46$, $p = 0.11$). (Note that “ p ” in this and subsequent figures represents the empirical significance level for the test result, or the probability of a poorer fit to the model by chance. When “ p ” approaches unity, the fit is improbably good; when “ p ” approaches zero, the fit is improbably bad.) *Bottom: Test of the Uniform distribution of arrival times. 3c:* Frequency histogram of arrival times (grouped into 20 segments) for the anticoincidence background data, showing a good fit to the uniform distribution ($p = 0.75$). *3d:* Empirical cumulative distribution function (cdf) of arrival times, utilizing the complete data from 585 individual events, showing a good fit ($p = 0.84$). This type of test can only be made when individual pulse arrival times are available, but it can often provide considerably more insight than tests made on aggregated data.

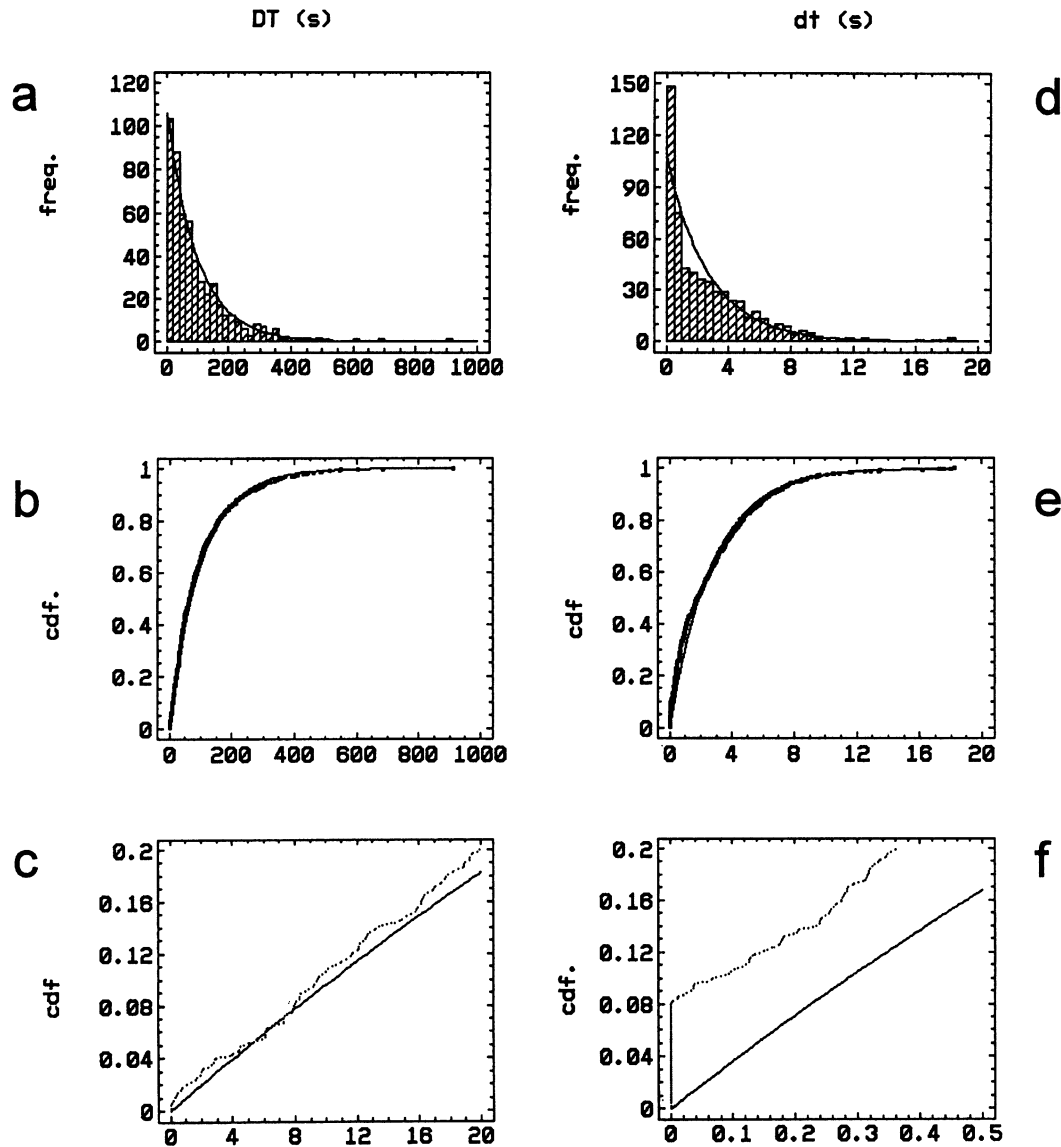


Fig. 4. Internal tests of the Exponential distribution of inter-arrival times: (DT, left) between anticoincidence background events, and (dt, right) between anticoincidence and preceding coincidence events. **4a**: frequency histogram (50 classes) for DT inter-arrival times between 0 and 1000 s; mean = 100.7 s, equivalent to a mean background rate of 0.60 cpm (total for the two GM counters); fit is good ($p = 0.40$). **4b**: empirical-cdf of DT inter-arrival times, utilizing the complete data from 585 individual events, showing an acceptable fit ($p = 0.13$). **4c**: expanded cdf for the first, 20-s class, better displaying fine structure in the differences between the theoretical and empirical curves. **4d**: frequency histogram (40 classes) for dt inter-arrival times between 0 and 20 s; mean = 2.72 s, equivalent to a mean rate of 22.0 cpm; fit is not good ($p = 0.9 \times 10^{-4}$), showing, for example, a 50-count excess in the first 0.5-s class (histogram bin) and a 25 count deficiency in the third class. **4e**: empirical-cdf for the complete set of individual dt inter-arrival times, again with a poor (Kolmogorov-Smirnov) fit ($p = 1.2 \times 10^{-4}$). **4f**: expanded cdf for the first, 0.5-s histogram bin, showing a major departure from the null hypothesis, with a set of 46 dt intervals $< 500 \mu\text{s}$, contributing about an 8% excess to the anticoincidence background rate.

Unique Insight Gained from the Anticoincidence-Coincidence Inter-Arrival Times (dt; Fig. 1b).

For low-level anticoincidence counting the dt time series has something special to offer. Referring again to the individual pulse data stream of 29 April, we show the exponential distribution tests in Figure 4 (d–f), using dt in place of DT —with a surprising result. The set of 585 anticoincidence background events, which previously showed good consistency with the presumed Poisson process, now exhibit a *major* discrepancy. The conclusion is that the background events, as observed, are not at all consistent with a Poisson process. The nature of the departure, unclear from Figure 4 (d,e), becomes apparent when the display is expanded to show very short dt (<1 ms) behavior (Fig. 4f). We see about an 8% excess (46 events) of unexpectedly short coincidence-anticoincidence inter-arrival times.⁸ The excessive events are, in fact, “afterpulses”; they reflect the physics and chemistry of the GM counting process, *not* characteristics of the background radiation. A considerable literature exists on this subject, and its relevance to detection and distributional phenomena in low-level counting are treated elsewhere (Currie *et al.* 1997). The bottom line, however, is that nearly 1 in 10 of the anticoincidence background events observed in the 29 April experiment were *not real background events at all*, but artifacts associated with the operation of the GM counting tube. It is important to note that the 46 artifactual events were included among the anticoincidence pulses that *passed* the three tests for the Poisson process, discussed in the preceding paragraph.

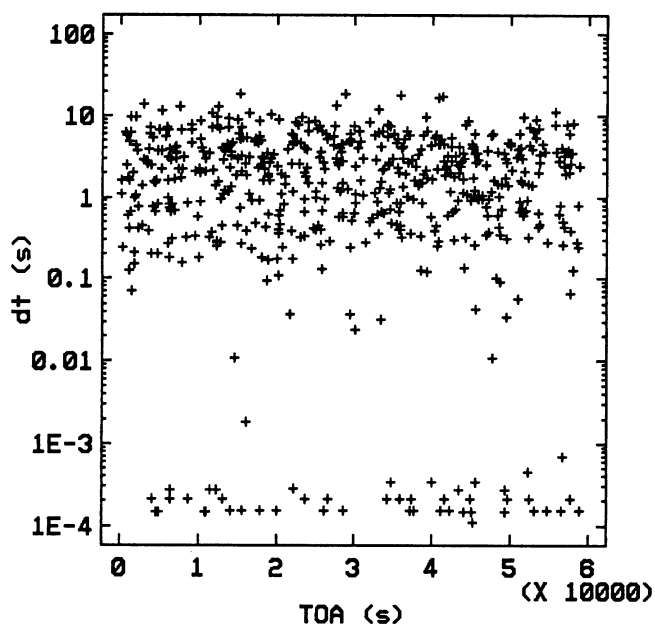


Fig. 5. *Dual distribution plot.* By plotting $\log dt$ vs. the arrival time we can assess (visually) the dual distributional character of the complete array of the individual background events. This is a very powerful means to discover unsuspected behavior in a single diagram, that here presents information contained in Figures 3 and 4 with no sacrifice in resolution. It also shows what was hidden in the univariate plots: that the afterpulses appear to be more or less uniformly distributed in time.

Dual Distribution Plot

To provide a powerful graphical means for detecting spurious pulses and for assessing, simultaneously, consistency with *both* the uniform and exponential distributions, we devised a “dual distribution” plot. This is shown in Figure 5, with TOA (abscissa) and $\log dt$ (ordinate), for the individual pulse data of 29 April. This method of display shares the full individual event resolution advantage

⁸Given the mean “ dt ” inter-arrival time of 2.72 s, it is clear that 8% of the pulses are very unlikely to have $dt < 1$ ms by chance, as the expected percentage would be just $100 \times (1 - \exp(-0.001/2.72)) = 0.037\%$.

of the empirical cumulative distribution functions (Figs. 3, 4), but it does so for both the TOA data and the dt data at the same time. Introduction of the log transform has the merit of exposing data in both tails of the dt distribution. From Figure 5, we can see at a glance that there are two distinct categories of inter-arrival time data: those for which dt is generally >10 ms, and those for which it is generally <1 ms. The two categories are, of course, the “proper” Poisson process background events, and the afterpulses, respectively. Two additional points are prominent in the dual distribution plot—namely, 1) that there is little to be seen for $dt < 150 \mu\text{s}$ (ordinate), and 2) that *both* proper and spurious background events appear to be uniformly distributed in time (abscissa). The first observation illustrates the effect of the GM tube deadtime; the second, “visual” conclusion was verified by numerical significance testing, with $p(\text{K-S}) = 0.84$ for the proper background events and $p(\text{K-S}) = 0.46$ for the spurious events (afterpulses). This is a rather interesting conclusion, because it means that both types of events constitute random time series (“renewal processes”), but only when we isolate the proper background events do we have a “Poisson process” (with respect to the entire coincidence, anticoincidence time series). Another observation concerning the afterpulses is that they represented comparable fractions of the background events in each of the paired counters: 9.2% and 8.5% averaged over the entire set of (external) counting periods.

Two Special Cases—Shocked and Stressed Counters

Background distributional properties were evaluated also for counting tubes that had been exposed to “shock” and “stress”—conditions that occasionally, inadvertently, arise in low-level counting. (Examination of these two special cases was motivated also by the experimental design principle of ruggedness testing [Massart *et al.* 1988: Chap. 6].) We use the term “shock” to refer to the momentary application of excessive high voltage, and “stress” to refer to the continued application of moderately high operating voltage, near the end of the GM plateau. Figure 6 shows distributional results from these experiments. The *shock* applied, in the first experiment, was the momentary, inadvertent application of the gas proportional Guard counter high voltage (2526 V) to the GM counting tube whose normal operating voltage is 1260 V (Fig. 6a,c); following the momentary shock the counter was run in background mode at its normal operating voltage. The *stress* applied, in the second experiment, was an increased operating voltage of 1500 V, near the end of the GM plateau (Fig 6b,d). The upper portions of the figure (Fig. 6a,b) display pulse arrival time histograms for testing the hypothesized uniform distribution. The lower portions show the corresponding dual (log dt, TOA) distribution plots displaying the complete individual pulse resolution. Numerical significance testing is not at all needed in this case; both histograms show marked deviation from the fitted, uniform distributions. Curiously, the average anticoincidence counting rates were similar (1.65 cpm and 1.70 cpm), both being some six and a half times the long term average background rates of *ca.* 0.26 cpm.

Two new phenomena are apparent in the plots. The shocked counter shows a characteristic relaxation (“decay”) curve, which has an initial first order time constant of *ca.* 30 min. Gradual return to the normal background rate took place over a period of about one day, after which the counter again performed well as a low-level counter. Except for the relaxation phenomenon, the pulse data stream reflected a random time series. The stressed counter, on the other hand, after a relatively small initial transient, maintained an increased average counting rate, in part as a result of a dramatic series of “bursts,” or time sequences containing relatively large numbers of closely spaced, anticoincidence events. When quite large bursts occur, they are prominently displayed in the upper histogram plot (Fig. 6b), but the lower, dual distribution plot (Fig. 6d) tells us more. Besides the large bursts containing hundreds of individual events, the log dt ordinate allows us to discern numerous smaller bursts containing 10 or fewer events. What is especially notable is that the intervals within the bursts are *not* primarily those characteristic of afterpulses (<1 ms); rather, they cover the full range from

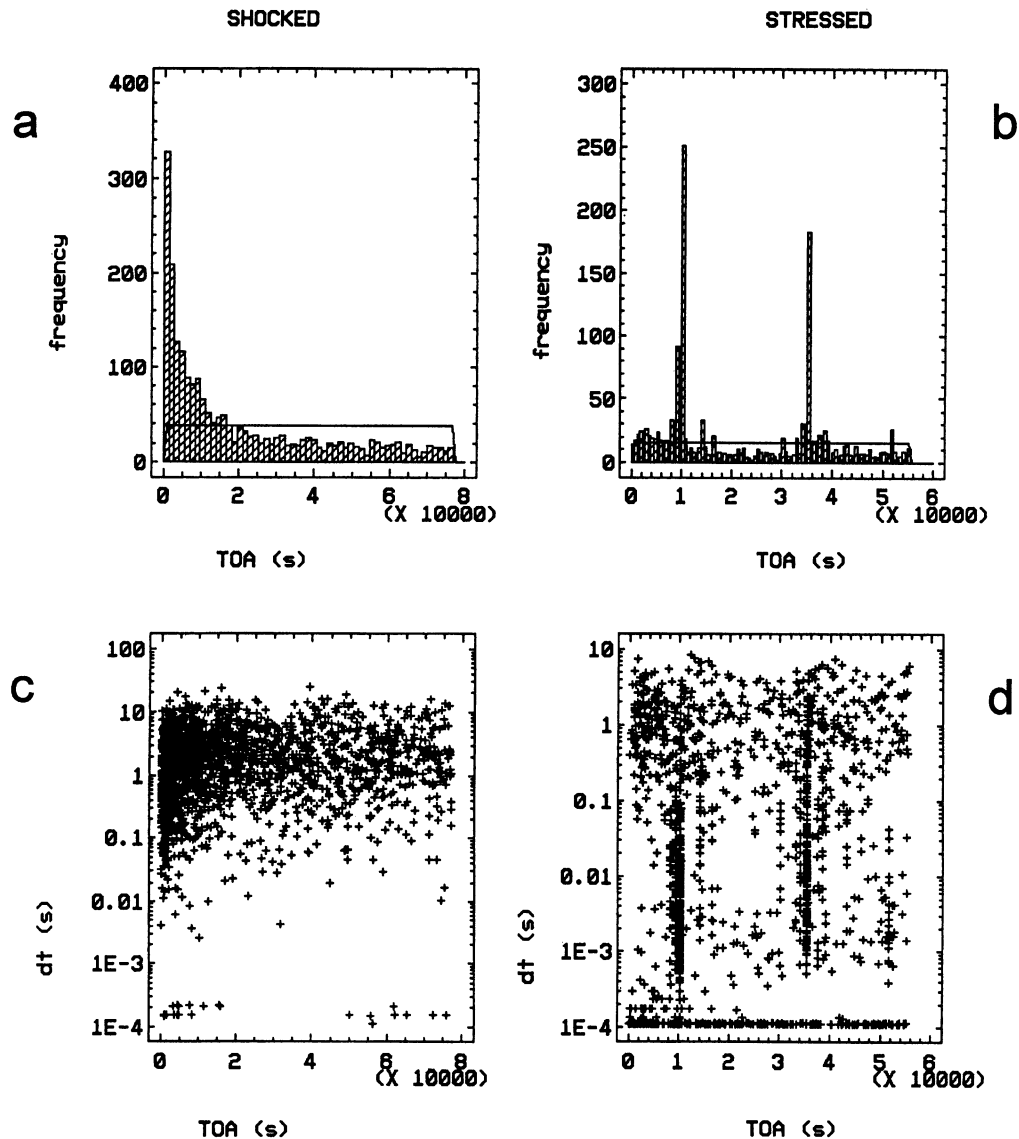


Fig. 6. Two special cases exhibiting marked departures from the Poisson process: counters exposed to “shock” (momentary excessive high voltage) and “stress” (relatively high operating voltage). Although average counting rates exceeded normal background levels similarly (more than a factor of six) in each case, the arrival time and inter-arrival time distributions were decidedly different. **6a** and **6b** display frequency histograms for individual anticoincidence pulse arrival times for the shocked and stressed GM counters, respectively. The shocked counter exhibits a transient relaxation (decay) process starting with a very high counting rate, and decaying with an initial time constant of *ca.* 30 min; the stressed counter shows generally low rates, marked by erratic bursts of anticoincidence counts with sudden onsets, very high instantaneous rates, and rapid decay (*ca.* 1 s). **6c** and **6d** are the corresponding dual distribution plots displaying the complete individual pulse data arrays. Here we see, for example, that 1) the transient behavior of the shocked counter is not linked to bursts or excessive afterpulsing, whereas 2) the stressed counter has a large and continued increase in afterpulsing (by about a factor of 12), plus pulse bursts of many sizes (pulses/burst) with intra-burst intervals ranging from <1 ms to 0.1 s or more.

ca. 1 ms to a fraction of a second. Nor do the bursts exhibit the uniform arrival time distribution of the afterpulses. Higher resolution examination of the bursts showed a sudden onset with instantaneous anticoincidence rates of ca. 1000 s^{-1} , followed by rapid decay (time constant of 1 s or less). The time interval between bursts is a bit erratic, and apparently dependent on both overvoltage and burst size. Extremes for the burst recurrence times observed ranged from a few minutes (Fig. 6) to a few days (normal operating voltage).

The burst phenomenon did not vanish at lower operating voltages, though it became relatively rare. Bursts of 3 or 4 anticoincidence pulses were occasionally seen, with intra-burst intervals in the same range of a few ms to a fraction of a second. This appears to be a counting system artifact that causes the background radiation, *as observed*, to differ from a Poisson process. It is noteworthy that the coincidence event data, corresponding to the anticoincidence data shown in Figure 6, remained well-behaved. Rates at the two voltages were $18.99 \pm 0.12 \text{ cpm}$ and $19.25 \pm 0.14 \text{ cpm}$, respectively. (Uncertainties shown are Poisson standard deviations.)

CONCLUSION

Apart from possible systematic variations in mean level (nonstationarity), low-level counting background radiation is commonly assumed to represent a random series of independent events that can be described as a Poisson process. Deviations from a Poisson process can be of considerable interest theoretically, and they may be of some consequence in planning extensive or high precision low-level experiments, and in estimating uncertainties of results. Use of a pair of matched low-level GM counting tubes, together with the NIST individual pulse analysis system, permitted us to perform external count rate experiments of serial and parallel background observations, as well as more powerful internal tests of the Poisson distribution of counts, the uniform distribution of arrival times, and the exponential distribution of inter-arrival times. The background radiation, viewed necessarily through the “eyes” of the (GM) counting system, showed several departures from the null (Poisson) hypothesis. The primary conclusions follow:

- The null hypothesis, that the low-level background radiation can be described as a Poisson process, *is inconsistent* with our observations using GM counting tubes.
- Separation of the “observed” (background radiation) from the “observer” (GM counting system) is not necessarily trivial nor completely possible (see footnote 5 above). Background radiation *as observed*, however, has direct relevance to the interpretation of low-level counting experiments.
- External tests of Poisson behavior (between results of extended counting periods) showed:
 - nonstationarity (trend in mean rate), especially with respect to coincidence background counts, as expected, due to the effect of barometric pressure on muon intensity;
 - excellent compensation for the nonstationarity by the online, paired counter technique, with the surprising result that the reproducibility of the net rate was “too good” (index of dispersion less than unity).⁹
- Internal tests of the arrival times and inter-arrival times of individual coincidence and anticoincidence background events revealed a number of departures from the ideal Poisson-exponential distribution:

⁹Nonstationarity compensation is to be preferred over the practice of using an “error multiplier” to account for a wandering mean background level, as the latter approach presumes the nonstationarity to be random and to have a known distribution.

- counting system deadtime (expected), which imposes a truncation to the realizable exponential distribution of inter-arrival times (Jordan and McBeth 1978). Although pronounced for GM counting, the matter of finite resolving time affects *all* measurements of individual events with radiation detectors.
- deviations from the expected constant GM pulse amplitude, in the form of “giant” pulses and an asymmetric distribution of small pulses extending from the mean pulse amplitude down to the discriminator threshold.
- afterpulses, of substantial abundance in the observed background radiation (8 to 10%), that *escaped detection* in the conventional tests of inter-arrival times between anticoincidence background events. Randomness of the GM background pulse data stream does not appear to suffer from the presence of the afterpulses, but the exponential distribution of inter-arrival times does, *i.e.*, we have a renewal process, but not a Poisson process. The inter-arrival time distribution of the afterpulses can have a pronounced effect of high accuracy low-level (interlaboratory) measurements.
- transient, counter relaxation (“decay”) phenomena following momentary exposure to excessive high voltage (“shock”).
- increased frequency and increased size of erratic “bursts” (mini-discharges) with increased operating voltage (“stress”); the burst phenomenon represents a major departure from the Poisson process, that benefits from an individual pulse analysis system to detect it at the lowest levels in background radiation measurements. The distributional character of the bursts is uniquely different from that of the afterpulses.
- Individual bursts showed very rapid transient behavior, with sudden onset and initial instantaneous “background” rates of *ca.* 1000 s⁻¹, followed by relaxation times of the order of a second.

Time constants for the several types of events in the background radiation as observed were: coincidence counts, 3.1 s; anticoincidence background counts, 3.6 min; afterpulses, 0.67 hr; giant pulses, 0.8 days; bursts, erratic from a few minutes to a few days. All of these pale, however, compared to the *ca.* 30-yr interval between investigations at NBS/ NIST on the validity of the Poisson process for counts obtained with radiation detectors (Curtiss 1930; Garfinkel and Mann 1968; this paper 1998).

REFERENCES

- Berkson, J. 1975 Do radioactive decay events follow a random Poisson-Exponential? *Journal of Applied Radiation and Isotopes* 26: 543–549.
- Cannizzaro, F., Greco, G., Rizzo, S. and Sinagra, E. 1978 Results of the measurements carried out in order to verify the validity of the Poisson-Exponential distribution in radioactive decay events. *Journal of Applied Radiation and Isotopes* 29: 649–652.
- Cook, G. T., Scott, E. M., Wright, E. M. and Anderson, R. 1992 The statistics of low-level counting using the new generation of Packard liquid scintillation counters. In Long, A. and Kra, R. S., eds., Proceedings of the 14th International ¹⁴C Conference. *Radiocarbon* 34(3): 360–365.
- Cox, D. R. and Lewis, P. A. W. 1968 *The Statistical Analysis of Series of Events*. London, Methuen & Co.: 285 p.
- Curtiss, L. F. Probability fluctuations in the rate of emission of α particles 1930 *Journal of Research of the National Bureau of Standards* 4: 595–599.
- Currie, L. A. *et al.* (ms.) 1997 Nature, impact, and spectroscopy of afterpulses in low-level counting systems.
- Currie, L. A., Gerlach, R. W., Klouda, G. A., Ruegg, F. C. and Tompkins, G. B. 1983 Miniature signals and miniature counters: Accuracy assurance via microprocessors and multiparameter control techniques. In Stuiver, M. and Kra, R. S., eds., Proceedings of the 11th International ¹⁴C Conference. *Radiocarbon* 25 (2): 553–564.
- Eijgenhuijsen, E. M. *et al.* (ms.) 1996 Design and development of a low-level counting system with individual pulse analysis.
- Garfinkel, S. B. and Mann, W. B. 1968 A method for obtaining large numbers of measured time intervals in radioactive decay. *Journal of Applied Radiation and Isotopes* 19: 707–709.

- Jordan, D. and McBeth, G. W. 1978 An experimental test of Müller statistics for counting systems with non-extending dead time. *Nuclear Instruments and Methods* 155: 557–562.
- Kaihola, L., Polach, H. and Kojola, H. 1984 Time series analysis of low-level gas counting data. *Radiocarbon* 26(2): 159–165.
- Kern, J. 1963 Paramètres de la décharge Geiger. *Helvetica Physica Acta* 36: 12–40.
- Massart, D. L. *et al.* 1988 *Chemometrics: A Textbook*. Amsterdam, Elsevier: 488 p.
- Mook, W. G. 1982 International comparison of proportional gas counters for ^{14}C activity measurements. In Stuiver, M. and Kra, R. S., eds., Proceedings of the 11th International ^{14}C Conference. *Radiocarbon* 25(2): 475–484.
- Narita, Y., Igarashi, R., Akagami, H. and Ozawa, Y. 1979 Suppression and utilization of spurious pulse occurrence in organic GM-counters. *Nuclear Instruments and Methods in Physics Research* 158: 161–168.
- Nicholson, W. L. 1966 Statistics of net-counting-rate estimation with dominant background corrections. *Nucleonics* 24: 118–121.
- Theodórsson, P. 1992 Quantifying background components of low-level gas proportional counters. In Long, A. and Kra, R. S., eds., Proceedings of the 14th International ^{14}C Conference. *Radiocarbon* 34(3): 420–427.

POSTSCRIPT

In response to requests from reviewers who are expert in statistics but unfamiliar with low-level counting, we offer here a very brief explanation of the technique, and its implications for vulnerability to, and detection of, spurious (after-) pulses. The basic principle is to use the time coincidences between discharges from the central, “sample” counter and an enclosing (concentric) “guard” counter, when both are triggered by penetrating external radiation, specifically cosmic-ray produced mu mesons. This provides a major reduction in background for the type of system employed here, because the vast majority of the background events are of this type (>98% for our system). It is for this reason that we have a *ca.* 60-fold reduction in background, from *ca.* 20 counts per minute (cpm) to *ca.* 0.3 cpm. Spurious, counter-generated events, which are relatively rare, are unlikely to occur simultaneously in both guard and sample counters, producing coincidence counts. However, such spurious events may be induced by *all* counts occurring in the sample counter—*i.e.*, *ca.* 20 per min; because of delay times between the inducing particle and the spurious discharge, such afterpulses will almost certainly appear as anticoincidence (background) pulses. That enhances both their impact, and their detectability *provided that* individual pulse “dt” inter-arrival time analysis can be employed. A further aspect of the counting experiment, that contributes to our null hypothesis, is that all pulses should have approximately the same amplitude, since the counters were operating as GM tubes.